Ecological Indicators 120 (2021) 106889

Contents lists available at ScienceDirect

Ecological Indicators

journal homepage: www.elsevier.com/locate/ecolind

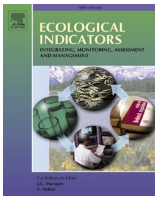

A new simple topo-climatic model to predict surface displacement in paraglacial and periglacial mountains of the European Alps: The importance of ground heating index and floristic components as ecological indicators

Stefano Ponti [a], Nicoletta Cannone [b], Mauro Guglielmin [a,*]

[a] Department of Theoretical and Applied Sciences, Insubria University, Varese, Italy
[b] Department of Science and High Technology, Insubria University, Como, Italy

ARTICLE INFO

Keywords:
Surface displacement model
Slope
Ground heating index
Permafrost degradation
Vegetation rooting depth
Ecological indication of movement

ABSTRACT

Landscape evolution is occurring at rapid rates in alpine areas in response to recent climate warming, also due to the susceptibility and the heterogeneity of these environments. Here we present a prediction model of surface displacements that takes into account both topographic and climatic variables. Observed points of surficial displacements have been associated to non-climatic (altitude, slope, solar radiation, till deposit type, deposit age, vegetation coverage) and climatic (days of snow permanence, ground surface temperature index, ground heating index, ground cooling index) variables through a general regression model in the European central Alps.

The model output shows the importance of slope and ground heating index (GHI) – an estimation of the amount of energy transferred to the ground, to predict surface displacements independently from the type of considered processes. In particular, the general regression model shows that steep zones with high GHI are more susceptible to undergo periglacial and paraglacial processes producing surface displacements. As expected, slope is fundamental to trigger processes such as gravitation, nivation, solifluction and their interactions. The results of our model emphasize the key role of GHI, highlighting the importance of climate in controlling the surface displacement. Indeed, in areas in which GHI is higher, the ground can remain snow free for a longer time and snow melting can be faster, the former favoring more runoff and slopewash, and the latter promoting the saturation of the deposits consequent to a higher intensity of solifluction and/or mass movements processes.

Within the study area, the sites with the largest displacements (>35 cm) were detected where permafrost degradation occurred since 1990. This permafrost degradation process could remain one of the main triggering factors of future surface displacements. Our results confirm that when movement involves material with coarse texture (pebbles and boulders) exceeding the rooting depth, only tolerant plant species can withstand the high movement rates. The areas where this can happen (like rock glaciers or screes) act as a physical barrier to grasslands species not adapted to surface displacements and trying to shift towards higher altitude in response to climate warming. However, plant species not considered as indicators of movement (such as graminoids), can develop also with large surface displacements in specific geomorphic conditions. Therefore, the combination of surface displacement type (deep vs surficial), material texture (fine vs coarse) and vegetation cover (high vs low) and floristic composition can be used as a valuable ecological indicator of movement.

Our results suggest that both landscape degradation and vegetation displacement can be rapid especially where the air warming was strong as in the selected study area.

1. Introduction

Large parts of the middle latitude mountains are no longer glaciated (Diolaiuti et al., 2011; Oerlemans, 2005; Paul et al., 2007; Zemp et al., 2008) and many others are rapidly becoming ice-free. In the frame of the current climate change scenario, the landscape is changing and

---

* Corresponding author.
E-mail address: mauro.guglielmin@uninsubria.it (M. Guglielmin).

https://doi.org/10.1016/j.ecolind.2020.106889
Received 2 November 2019; Received in revised form 15 August 2020; Accepted 25 August 2020

paraglacial and/or periglacial conditions are widespread. Despite an intuitive relation between climate and landscape changes, only few works have focused on the combined effects of climate change and landscape modelling (e.g., Coulthard, 2001; Tucker and Hancock, 2010). In middle or low latitude mountain regions the spatial variability is very high mainly due to the topography (Becker and Bugmann, 1997) and therefore even small changes in climate drivers as air warming or solar radiation increase, but also the degree of snow permanence or wind speed could have important effects on the landscape changes and on the related ecosystems at different scales (Chapin et al., 2008; IPCC, 2013). Moreover, land degradation at the micro-scale (from millimeters to decimeters) can exert an additional impact on ecosystems and on plant development. Indeed, land degradation, known also as “physical disturbance” or “disturbance”, (frost heave, frost creep or solifluction, rill erosion, pebble and boulder movements) has been known to cause species altitudinal shifts, changes in species composition, richness and productivity, and adaptations to surface movements (e.g. Cannone et al., 2007; Virtanen et al., 2010; Burga et al., 2004; Cannone and Gerdol, 2003).

The monitoring of widescale geomorphic processes at the micro-scale in high mountain environments is undertaken infrequently or seldom undertaken (e.g., Ballantyne, 2013; Harris et al., 1998; Matsuoka, 2006) and, in many cases, focuses on a single geomorphic process, such as: 1) solifluction (Ballantyne, 2013; Matsuoka, 2001a) and its relation to vegetation development (Draebing and Eichel, 2018), 2) needle ice (Grab, 2001; Nel and Boelhouwers, 2014; Ponti et al., 2018), 3) frost wedging (Matsuoka, 2001b; Tharp, 1987), 4) rill erosion (Cai et al., 2004; Govers, 1992), and 5) nivation (Ballantyne, 1985; Thorn and Hall, 2002). In order to improve knowledge of the spatial variability of the land degradation and surface dynamics, many studies tried to focus on coupling remote-sensing with geographic information systems (GIS) (Arenson et al., 2016; Kääb et al., 2003, 2014; Micheletti et al., 2015; Necsoiu et al., 2016; Westermann et al., 2015). In many cases, when coupled with a reliable data validation, the GIS approach provides a rapid solution for expanding the investigated area or generating models (Dymond et al., 2006; Lee, 2005; Marmion et al., 2008; Pradhan, 2010).

Several predictive/distribution models have been produced focusing on the susceptibility of certain areas to undergo slope processes (Bai et al., 2010; Brenning, 2005; Carrara et al., 2008; Das et al., 2010; Frattini et al., 2008; Komac, 2006; Messenzehl et al., 2017; Saito et al., 2009) or on periglacial processes (Hjort, 2014; Luoto and Hjort, 2004, 2005; Marmion et al., 2008). However, few of these studies integrate the models with climate (Aalto and Luoto, 2014; Fronzek et al., 2006; Hjort et al., 2007) or vegetation variables (Choudhary et al., 2017; Hjort, 2014; Miao et al., 2012; Miller, 2013) and do not always include importance of snow distribution (Guglielmin et al., 2003; Randin et al., 2009). Previous studies focused on the risk assessment but without a quantification of the physical processes within areas of potential slope-induced hazards (Pelletier, 2008; Baas, 2013). However, taking the quantification of the effects of slope displacement beyond just a probability is important as it could be treated as a quantitative risk assessment especially in mountainous areas without anthropogenic influence. These areas have already been recognized as highly susceptible to the recent climate change concerning the vegetation shifts/colonizations (Cannone et al., 2007; Gottfried et al., 2012; Keller et al., 2000; Theurillat and Guisan, 2001; Walther et al., 2005). Therefore, the role of surficial dynamics modelling could also be implemented in vegetation distribution models (Mod et al., 2016; Pfeffer et al., 2003; Räsänen et al., 2016; Zinko et al., 2005).

This work aims to:

i) produce a simple quantitative prediction model of surface displacement coupling/based on both the topographic and climatic information in an alpine area. For this aim, the dynamic prediction is not only treated as probability of occurrence, but also as numerical quantification, allowing the use of this model as predictor of surface displacements under future climatic scenarios;

ii) compare the predicted displacement with the permafrost distribution and the occurrence of plant species, in order to understand their relation and assess whether warming of the surface temperature would allow the upslope advance of competitive species that might threaten the specially adapted species to unstable ground in a context of future landscape change in that area.

2. Study area

The study area is located around Stelvio Pass (46°31′ N, 10°25′ E; elevation 2230–3094 m above sea level) close to the border between Italy and Switzerland in the Central Alps (Fig. 1).

The climate is characterized by a continental regime (Ceriani and Carelli, 2000), with highly variable values of precipitation due to the complex orography. Climate data for the period 1978–2015 from the nearest available meteorological station at Cancano (46°31.03′ N, 10°19.24′ E, 1948 m a.s.l., 9 km to E-SE) indicate a mean annual air temperature (MAAT) of + 3.3 ± 0.75 °C, with January being the coldest and driest month (−5.2 ± 1.8 °C; 38.9 mm) and July the warmest and wettest (12.2 ± 1.6 °C; 94.7 mm). Total mean annual precipitation is 810 mm, 56% of which falls between May and September. Snow can fall at any time laying continuously for 6 months, from mid November to May and reaching a mean maximum depth of 133 cm. Despite the patchy and discontinuous permafrost distribution (Guglielmin and Siletto, 2000; Guglielmin et al., 2001), at 3000 m the permafrost thickness exceeds 200 m (Guglielmin, 2004; Guglielmin et al., 2018).

The area is characterized by bedrock outcrops, as well as some

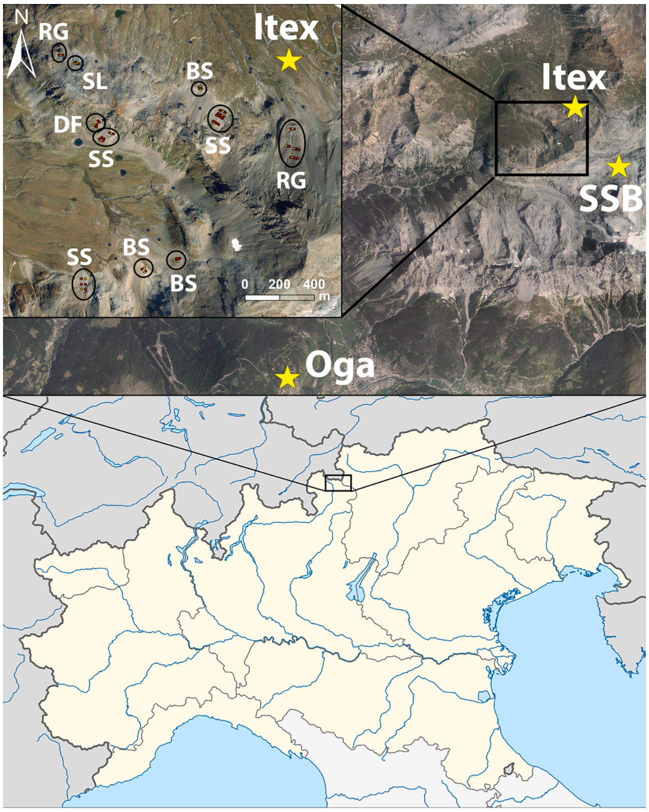

Fig. 1. The investigated area and the location of the automatic weather stations (AWS) (yellow stars). The colored dots are the monitoring points for the observed movements (red = training set, yellow = validation set). The monitoring locations are circled to indicate the landform type of the substrate: RG = rock glacier, BS = block stream, SS = scree slope, SL = solifluction lobe, DF = debris-flow.

Holocene till and talus deposits.

The Holocene glacial evolution of this area is not very well known. The Scorluzzo Glacier disappeared between 1937 and 1956 (Pelfini, 1992; Cannone et al., 2003).

Despite its limited extent (ca. 3 km^2), the area is rich in periglacial features including several types of patterned ground, solifluction lobes, scree slopes, protalus ramparts, block streams, debris-flows and at least two active rock glaciers (Guglielmin and Tellini, 1992).

The vegetation is typical of the alpine and nival belts (Ellenberg, 1988) and it was firstly mapped by Giacomini and Pignatti (1955) in 1953, then by Cannone et al. (2007). In the alpine belt, the dominant communities are the climax continuous alpine grassland (*Caricetum curvulae*) and the snowbeds (*Salicetum herbaceae*). In the nival belt, the most representative pioneer communities colonizing scree slopes are *Androsacetum alpinae*, *Oxyrietum digynae* and *Luzuletum spadiceae*.

At the elevations of the study area, the effects of anthropogenic land use change on vegetation are mostly negligible (Keller et al., 2005) with extensive summer pasturing being the only anthropogenic land use in our study area (Cannone et al., 2007; Malfasi and Cannone, 2020).

3. Material and methods

3.1. Surface data

Topographic information were obtained from the digital elevation model (DEM) of the study area available of the two snow-free periods (2015 and 2016) (5 m of resolution; http://www.cartografia.servizirl.it/arcgis/services/wms/DTM5_RL_wms/MapServer/WMSServer) in ArcGIS 10.3, from which were developed the slope map and the solar radiation maps (through the Area Solar Radiation tool), subsequently averaged to produce a single mean solar radiation map. The elevation ranges between 2320 and 3094 m a.s.l., while slope ranges between 0 and 72°, with the steepest areas corresponding to the rockwalls. The cumulative solar radiation of the snow-free period ranges between 10^5 to $1.2*10^6$ Whm^{-2}, with the lower values occurring on the north-facing slopes, and the higher solar radiation on the south-facing slopes and almost flat areas, as expected.

The new geological map by Montrasio et al. (2012) was re-classified for the deposit type and age rasterized with a resolution of 5 m. All the quaternary deposits are classified according to their age, in respect to the Little Ice Age (LIA), that occurred in this sector of the Central Alps sometime between 1580 and 1834 CE in this area (Guglielmin et al., 2001, 2018; Cannone et al., 2003) (Table 1). The deposits Post-LIA are quite rare and completely free of any soil coverage, while in the LIA areas only discontinuous soil occurs, whereas in Pre-LIA areas soils are often well developed with spodosoils that can exceed 50 cm of thickness. The age of the deposits is a proxy of their weathering and of the stability of the surfaces, while their typology (glacial till, slope deposits etc.) gives an indication of their average grain size (till generally sandy vs. alluvial generally gravelly) and of their selection (alluvial well selected vs till massive). Among the different deposit typologies, till is the most widespread, while scree slopes are concentrated at the foot of the rockwalls.

The vegetation map was obtained according the two previous vegetation maps existing for the area (Giacomini and Pignatti, 1955; Cannone et al., 2007). Continuous vegetation is abundant in flat areas at mid to low elevations, while it becomes discontinuous in proximity of streams or at the foot of scree slopes and at the higher elevations.

Table 1
Classification of the characteristics deriving from the geological and vegetation map. Classes are represented by the numbers at the first row. LIA refers to "Little Ice Age".

	1	2	3
Age of Deposits	Post-LIA	LIA	Pre-LIA
Deposit Type	Glacial till	Slope deposit	Landslide deposit
Vegetation Coverage	Bare Ground (<5%)	Discontinuous (5–50%)	Continuous (>50%)

To analyse the relations between surficial displacement and plant species was used 50 relevés performed in 2013 (Cannone et al., in prep.).

The bedrock outcrops were not considered in the model because these areas are generally not vegetated.

The measurements of surface displacements were added to the analyses as point data that represent the maximum displacement (cm) of each ten-meter sector of longer painted lines transversal to the flow direction of the landforms. For this, the normal shift of painted clasts from their original position was measured between 06 and 11-2014 and 06-11-2016. A total of 85 points spread on 2 rock glaciers, 3 scree slopes, 3 block streams, 1 solifluction lobe and 1 debris-flow were selected. The outliers of the dataset were removed to obtain a training set (57 points) and a validation set (21 points). This method follows the "random partition" of Chung and Fabbri (2003), with the exception that the selection of the validation set was not done randomly but by choosing 2–3 points placed at different altitudes on each landform to better represent all the landforms occurring in the modelled area.

3.2. Climatic data

Climatic data refers to air temperatures and snow distribution during the study period that was based on the availability of cloudless snow maps from 06 to 11-2014 to 06-11-2016. Not all the daily snow maps, derived from MODIS at a resolution of 250 m (Notarnicola et al., 2013a, 2013b), were used for this study, but an average of one snow map per week was a good compromise to avoid cloudiness and maintain dynamics of snow cover variations. Unfortunately, better resolution (30 m) images from Landsat have not been useful due to the high cloudiness of the images during the study period in the examined area.

The first step was to build a detailed map of air temperature occurring at each pixel (5 × 5 m) of the DEM. Secondly, the periods of the 2-year study have been defined in terms of snow coverage as shown in Table 2, assuming that the snow presence insulates completely the ground from the air temperature fluctuations (although we are conscious that the snow pack should be at least 80 cm thick to exert this complete insulation, i.e., Guglielmin et al., 2003).

The mean air temperature of the different periods was calculated from data series belonging to the 3 closest available automatic weather stations (SSB = 3000 m a.s.l., Itex = 2616 m a.s.l. and Oga = 2295 m a.s.l.). Subsequently, a linear regression was calculated between mean air temperatures for each defined period and the elevation of the correspondent stations allowing to extrapolate maps of mean air temperatures (all of them with $R^2 > 0.75$ and $p < 0.05$) for each pixel of the examined area for all the defined periods.

The third step was to generate the snow-free maps for each defined period: the sum of the snow-free days was computed for each pixel obtaining maps of the snow-free duration for each defined period. Finally, these snow-free maps were multiplied by the mean temperature of each correspondent defined period, thus obtaining the maps of Ground Surface Temperature Index (GSTI) expressed in °C day.

Table 2
Annual climatic division based on the snow presence and the mean daily air temperature. Each year was divided into four periods (Snow Cover, Melting, Freezing, Snow-free). Freezing period can occur also more than one time per year as happened in 2016 when both at the end of the snow cover (SCT) period and at the snow-free period (SFT) some days of freezing occurred.

Periods	Snow coverage (%)	Mean daily air temperature (°C)
Snow cover (SCT)	> 90	<0
Melting (MT)	< 90	>0
Freezing (FT)	< 90	<0
Snow-free (SFT)	< 10	>0

Moreover, thawing degree days (TDD) and freezing degree days (FDD) (Carter et al., 1991) were calculated for each period similarly to the air temperature. Mean TDD and FDD of the different periods have been calculated at the 3 weather stations and the linear regression ($R^2 > 0.75$ and $p < 0.05$) between elevation and TDD/FDD used to produce the corresponding maps. TDD and FDD values at each 5 m cell were multiplied by the snow-free days for each period, thus obtaining the maps of Ground Heating Index (GHI = snow-free days * TDD) and of Ground Cooling Index (GCI = snow-free days * FDD).

3.3. *Statistical analyses*

All the map operations described above and the spatial analyses of the vegetation relevés were conducted using the raster calculator tool in ArcGIS 10.3 (ESRI, 2011) and the spatial analyst tool.

From all the maps of the variables listed in Fig. 2, at each of the 57 training points both categorical and continuous data were extracted and used to run a general regression model (GRM) (Hill et al., 2006) in order to select the dominant variables with a backward stepwise option through the software STATSOFT©. In order to satisfy the normal distribution condition for the GRM input, all the continuous variables were square-root transformed. The GRM with backward stepwise option was applied to the training set considering all the values extracted at each point from the maps listed in Fig. 2 as independent variables and the observed values of surface displacement as dependent variables.

Afterwards, the calibration and the validation of the observed vs. predicted displacements were tested with the statistical descriptors listed in Willmott (1981). A flow-chart of the utilized variables is shown in Fig. 2.

The statistical analysis conducted on the vegetation species associated to surface displacement (which was recorded in the field during the study period) were conducted in STATSOFT© by removing displacement outliers through a graphical representation in the non-parametric section.

4. Results

Snow persistence ranged between 159 and 262 days per year. In general, snow persistence lasted longer at higher elevations although sometimes at lower altitudes snow persistence was longer in depressed and shady areas. GSTI for FT (ranging from 5.7 to 98.7 °C day) shows low values for higher elevations, even though the minimum is not reached at the most elevated place. GSTI for MT (ranging between 0.6 and 140 °C day) and SFT (ranging between 233 and 363 °C day) follows an inverse altitudinal pattern with the lowest values at higher elevations and north-facing slopes.

The GHI and the GCI are also both strongly controlled by DEM, although the range of variability is much wider for GCI (between $-2.39\ 10^6$°C day^2 and $-0.56\ 10^5$ °C day^2) respect in to the GHI, that ranges between $1.24\ 10^6$°C day^2 and $16\ 10^6$ °C day^2.

The GRM provided a statistically significant and good result ($R^2 = 0.45$; $p < 0.001$; $F = 22.8$).

According to the GRM, Slope and GHI are the most important statistically significant drivers of surface displacement (Table 3). Moreover, the model indicated that there is a direct linear relationship between Slope, GHI and Surface Displacement as expressed by the Eq. (1).

$$\sqrt{[\text{Predicted Surface Displacement (cm)}]} = 2.02*\sqrt{(\text{Slope})} + 0.03*\sqrt{(\text{GHI})} - 47.10 \tag{1}$$

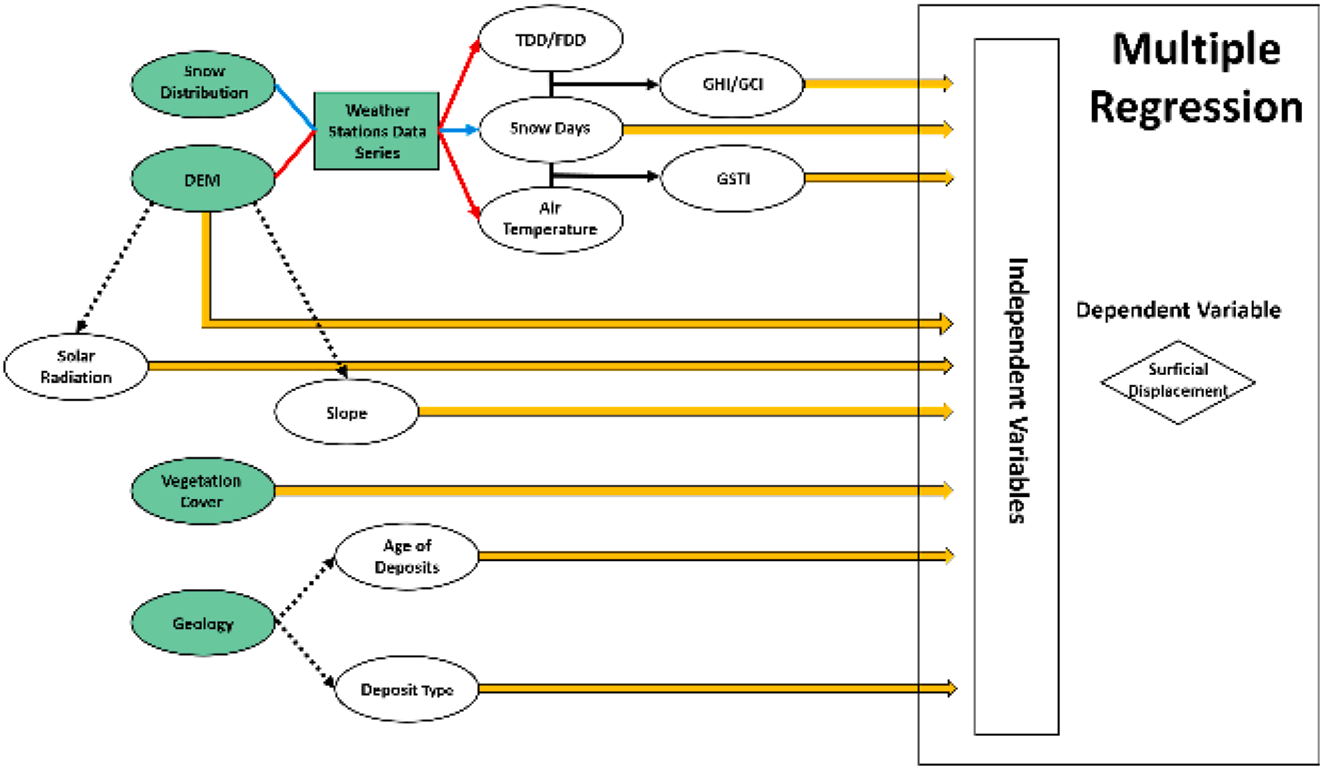

Fig. 2. Flow chart representing the calculation conducted for the general regression analysis. Raster maps are represented with ellipsis while climatic data series with a square. In green are shown the data sources (Weather stations data series, MODIS images for snow distribution, DEM, Vegetation Cover and Geological Map). The maps derived by raster data sources are linked with dashed black lines; Solar radiation and Slope derived from a parental map calculation in ArcGIS, while Age of Deposits and Deposit type derived from a re-classification of the geological map by Montrasio et al. (2012), TDD /FDD and air temperature derived from DEM (see red arrows) and weather data series while the number of days with snow cover derived from MODIS snow distribution and DEM (see blue arrows). Finally, from the interactions of Snow days and Air temperature or TDD/FDD maps derived GSTI and GHI/GCI that are used as independent variables together with all the other maps linked with yellow arrows. The rhombus (surficial displacement record) indicates the dependent variable of the general regression analysis.

Table 3
Statistically significant variables characteristics as outputs of the general regression analysis. β = standardized regression coefficient, F = ANOVA F-value.

	β	F	p-value
Intercept		9.0	0.004
Slope	0.57	31.9	< 0.001
GHI	0.26	6.45	0.014

By applying the Eq. (1) at the whole study area (Fig. 3), we predicted a displacement ranging between 0 and 170 cm for the entire period of the two selected years, with an average of 17.1 cm. The model predicts as highly dynamic areas the zones at lower elevation (<2500 m a.s.l) where both slope and GHI are high, such as the northernmost part of the study area, where solifluction lobes, terraces, rock glaciers and scree slopes occur, while the most elevated part of the examined area shows the lowest values of surface displacement. Intermediate values occur at the steepest parts at the foot of the rockwalls where the finest sediments prevail in the scree slopes.

The relatively low root mean square error (RMSE), the greatest part of which is systematic ($RMSE_S$) and the d values close to 1 suggest a good predictability of the model (Table 4), while the model fitting (R^2) does not show a very high value (0.42) but it is statistically significant.

Concerning the relations between plant species and the modeled surficial displacements, in Fig. 4 it is possible to identify the ranges of tolerance for all the species directly affected by displaced clasts (displacement-tolerant species) during the study period, with the occurrence of two ecological clusters (0–35 and >35 cm).

In the model area, 50 vegetation relevés were conducted in 2013 in the model area, of which 41 relevés were associated with a modelled surface displacement of 0–35 cm and the nine remaining with the >35 cm class. The relevés associated with the largest displacements were representative of three different case conditions and different geomorphic processes. I) Areas with surface displacement depth exceeding the root depth and fine material prevailing at the surface, such as on active rock glaciers: here the vegetation creates floating patches, and is characterized by high coverage and dominance of graminoids (*Luzula alpino-pilosa* (Chaix) Breistr., *Poa alpina* L., *Carex curvula* All., *Anthoxanthum alpinum* Honda, *Agrostis alpine* Scop.) (Fig. 5A). II) Areas with the surface displacement being deeper than the root zone, but with prevailing coarse material, such as on active rock glaciers or at the foot of screes. Here the vegetation is not able to create patches and a few species are able to withstand the high displacement rate, therefore the vegetation is characterized by low and discontinuous coverage and by the selection of species tolerant to high movement (such as *Geum reptans* L., *Cerastium uniflorum* Clairv., etc.) (Figs. 4 and 5B). III) Areas with surface displacement being surficial, as in the case of slope wash or frost creep (such as the apex of screes): the vegetation is characterized by small discontinuous patches with high cover and dominated by consolidator species (such as graminoids), creating small steps able to resist being buried by fine material (Fig. 5C).

5. Discussion

5.1. Model parameters

Several models have been developed addressing single geomorphic processes in the periglacial environment (French, 2007), such as rock falls (e.g., Messenzehl et al., 2017), solifluction and cryoturbation (e.g., Hjort, 2014), palsa mires (e.g., Fronzek et al., 2006) and patterned grounds (e.g., Luoto and Hjort, 2004). Only in few cases have models (i.e. Aalto and Luoto, 2014) focused on different processes involved in surface disturbance. Our model confirms the results of Aalto and Luoto (2014) in which the importance of incorporating climate and local (soil, vegetation) predictors into models at the landscape level was underlined. Moreover, in our case the combination of climate and local predictors are useful to model the surficial displacement independently by the different types of processes or landforms considered. Among the factors that we took into account, it is remarkable that the grain size of the sediments apparently does not play an important role, probably due to the generally coarse size of the sediments occurring in the area (and, in particular, where the monitoring points are located).

On the contrary, slope is a relevant parameter, as could be expected. Indeed, all the geomorphic processes that characterize the mountain belt depend on gravitational forces and, therefore, on slope (French, 2007; Harris et al., 2001; Harris and Smith, 2003; Matsuoka, 1998, 2001a). In particular, in the mountain areas of middle and low latitudes, slope processes could involve solifluction (Benedict, 1970; French, 2007;

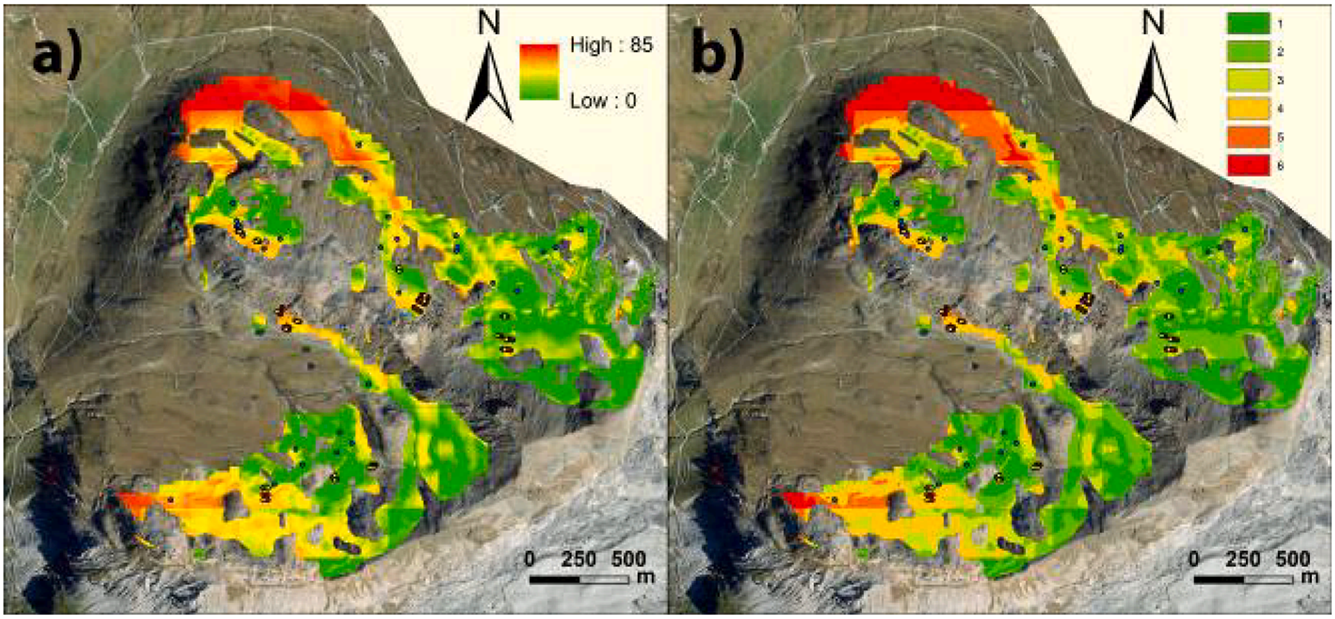

Fig. 3. Graphic visualization of the final model derived (Surface Displacement, cm) from the general regression equation. a) stretched model; b) classified model: 1 = 0–1 cm, 2 = 1–5 cm, 3 = 5–10 cm, 4 = 10–20 cm, 5 = 20–35 cm, 6 = >35 cm for the whole analysed period. Red dots indicate the training set, yellow dots indicate the validation set.

Table 4
Statistical descriptors useful to assess the quality of the model, both for the calibration (training) and the validation set. The descriptors follow what listed in Willmott (1981).

	R^2	Slope	Intercept	Mean O	Mean P	S_o	S_p	$RMSE_s$	$RMSE_u$	RMSE	d
Calibration	0.42	0.27	9.67	20.48	15.27	28.77	12.19	21.37	9.22	23.27	0.64
Validation	0.56	0.35	6.41	17.67	12.64	28.23	13.33	18.53	8.66	20.45	0.72

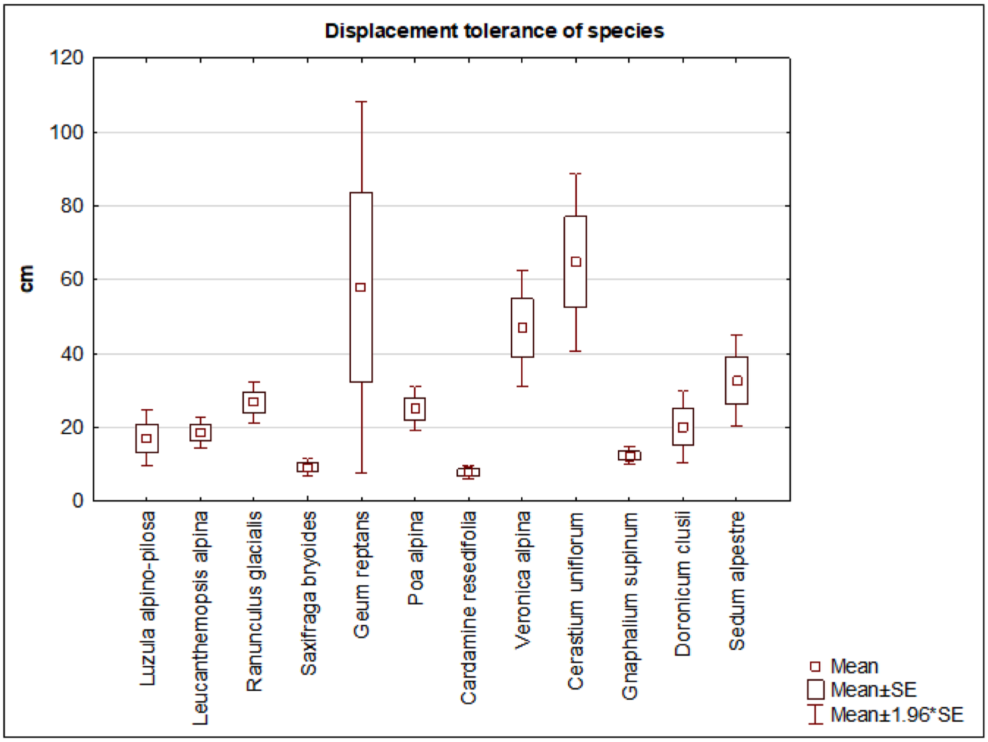

Fig. 4. Plant species associated with each recorded surface displacement during the study period. The box and whisker plots show the tolerance of the species to the surface displacement in terms of mean and standard error (SE). It is noticeable that many species have similar means or ranges and that a clusterization is visible for displacements as 0–35 and > 35 cm.

Goodfellow and Boelhouwers, 2013; Matsuoka, 2001a), gravitation (Luckman, 1976; Statham, 1976; van Steijn et al., 2002), nivation (Ballantyne, 1985; Thorn and Hall, 2002), periglacial and cryotic processes, and their interactions (Haeberli et al., 2006; Kääb et al., 1997; Pérez, 1993; Rixhon and Demoulin, 2013).

The higher relevance of slope in our model in respect to other models, like for example in Aalto and Luoto (2014), is probably due to the main periglacial processes considered by the authors like solifluction or cryoturbation generally developing on lower slopes.

Beyond slope, the second statistically significant factor is the GHI, showing a positive relation with the surface displacement. Therefore, the areas where snow is absent in combination with temperature >0 °C lasting for several days are characterized by a higher probability of surface displacement, possibly related with higher liquid precipitation, consequent runoff or slopewash (Thorn and Hall, 2002), infiltration in the soil, as well as evapotranspiration (desiccation) (van den Bergh et al., 2013; Wieser et al., 2008). Moreover, it is also possible that in these areas snow melting can occur faster inducing the saturation of the deposits, favoring the solifluction processes.

In periglacial belts like the examined area we should take into account permafrost occurrence in order to quantify its relation with land degradation. For the examined area we decided to use the only available permafrost map of the European Alps which includes the study area (Boeckli et al., 2012a, 2012b). Using this map we predicted a probable overestimation of the permafrost extent because it is based on climatic data referred to the period 1961–1990 and, therefore, does not take into account the more recent warming (Boeckli et al., 2012a). Indeed, the recent warming in the examined area is really strong, as demonstrated by Guglielmin et al. (2018) in correspondence of SSB (Fig. 1; 3000 m a.s.l.), where, between 1990 and 2011, an abrupt GST (ground surface temperature) warming exceeding >0.8 °C per decade was recorded. According to these data, it is reasonable that the permafrost areas mapped by Boeckli et al., 2012a, 2012b as “less probable” and “probable” could be actually permafrost-free or strongly degradated (Fig. 6a). The more unstable areas and the maximum recorded rates of displacements are located in the areas classified with “less probable” permafrost (classes 5 and 6, Fig. 6b and Table 5). Notably, the areas with the greater displacements classes (5 and 6) are all located below the −1 °C isotherm (2622 m a.s.l.) for the period 1978–1990 (Fig. 6), in areas where permafrost could occur until 1990. These results suggest that the permafrost degradation occurred since 1990 (and probably still ongoing below the −1 °C isotherm placed at 3000 m a.s.l. during the study period) and could be one of the main triggering factors of surface displacements. On the other hand, further investigations are needed to address this issue and assess where permafrost degradation is still ongoing or completed.

5.2. Ecological implications

Vegetation cover does not seem to be important as a model parameter, however vegetation could be treated as an ecological indicator of the surface displacement with reference to specific processes, for

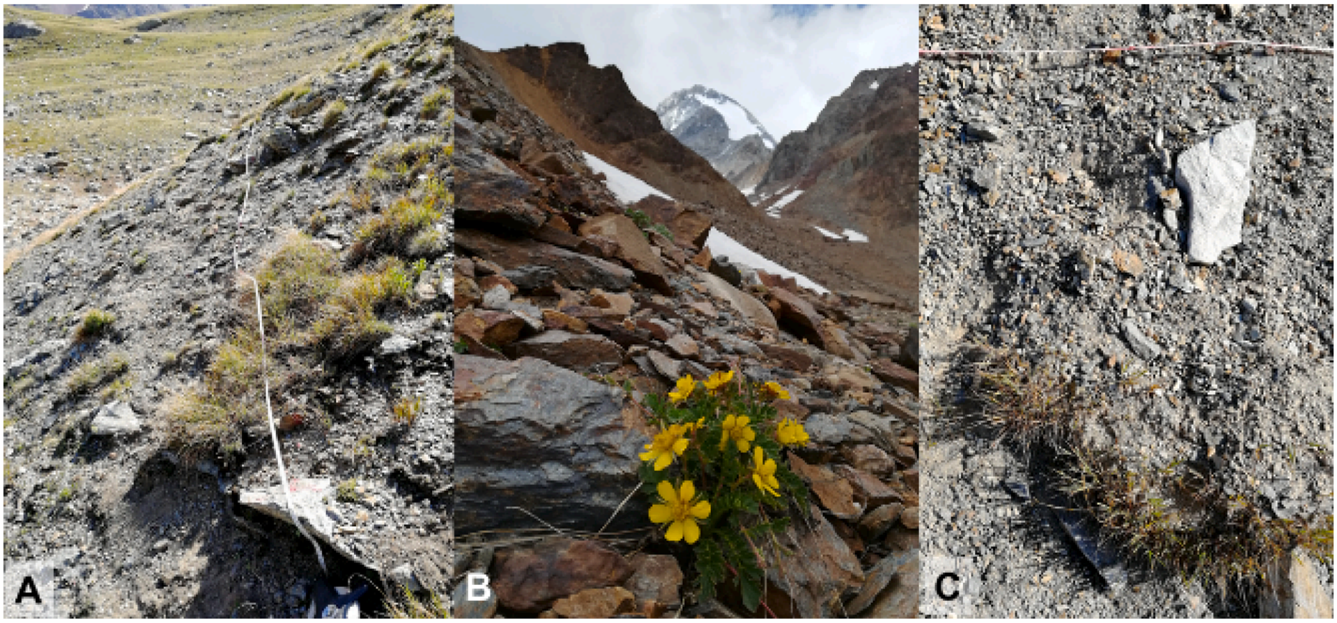

Fig. 5. Examples of the relations between vegetation and high surface displacements. A) high coverage vegetation floating patches/turve dominated by graminoids (*Luzula alpino-pilosa*, *Poa alpina*, *Carex curvula*, *Anthoxanthum alpinum*, *Agrostis alpina*) on an active rock glacier with the largest displacements exceeding the rooting depth and surficial fine material; B) discontinuous low coverage vegetation dominated by movement tolerant species such as *Geum reptans* and occurring where the displacement depth exceeds the rooting zone with coarse material such as at the foot of screes; C) small vegetation patches with high coverage of consolidator species (mainly graminoids) creating steps able to withstand the burial of fine material triggered by surface displacements, as in the case of the apex of screes.

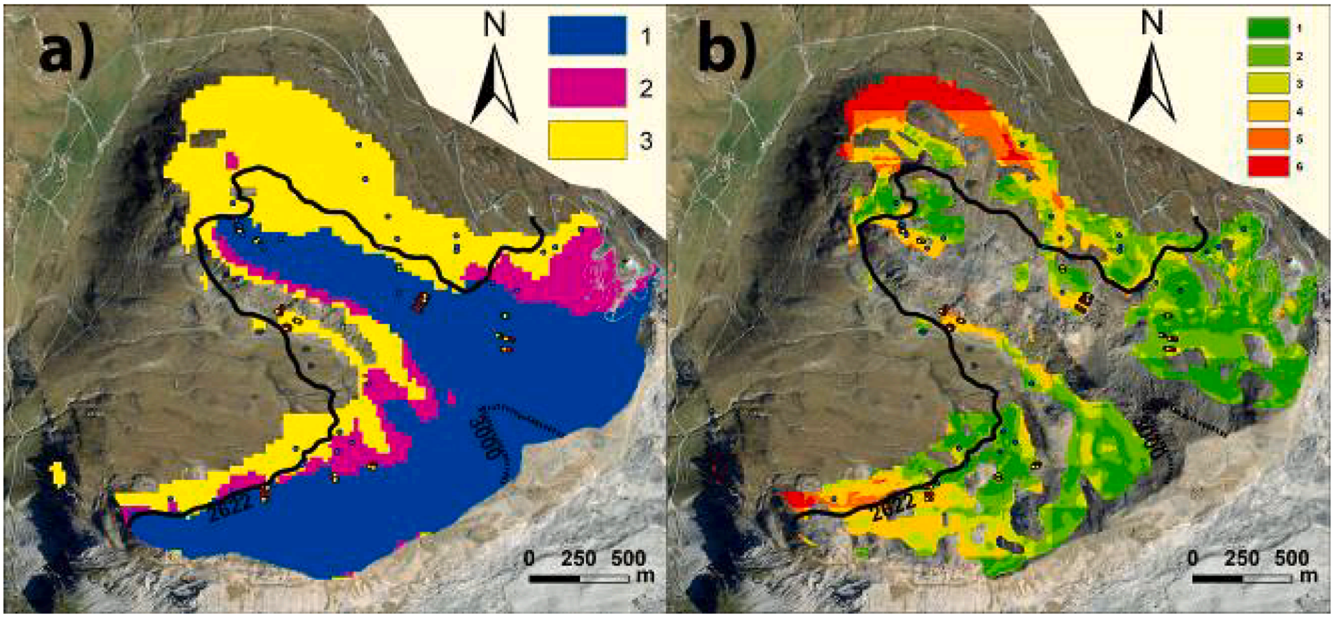

Fig. 6. Comparison between permafrost distribution (a) and the surface displacement model (b). Permafrost classes refer to: 1) present (blue), 2) probable (pink), 3) less probable (yellow) (Boeckli et al., 2012a). The two isolines indicate the elevation of the mean air temperature as isotherm −1 °C (2622 m a.s.l.) for the period 1978–1990 (solid line) (the closest available to Boeckli et al. (2012a) (1961–1990) and for the study period (dashed line) (3000 m a.s.l.).

Table 5
Percentage of pixels that match permafrost and displacement classes with general statistics of the modelled displacement.

	Displacement statistics (cm)		
Permafrost	Max	Mean	Std
Present	34.60	4.35	4.91
Probable	45.26	4.09	5.59
Less probable	85.31	14.42	16.80

instance, response to surface erosion (Miao et al., 2012; Stanchi et al., 2013), predictor of landslides (Miller, 2013), indicator of landslide relative age, detachment patterns and recolonization patterns (Cannone et al., 2010).

The use of vegetation cover did not produce good results in our modeling, due to different reasons. First of all, we used classes of coverage (Cannone et al., 2007) and not the spatial distribution of single plant species indicators of surface instability, such as *Cerastium uniflorum*, *Geum reptans* or *Saxyfraga bryoides* (Cannone and Gerdol, 2003;

Burga et al., 2004).

This is mainly due to the difficulty to produce a vegetation map at the species level at the examined scale due to the scarcity of mono-specific detectable patches: indeed, even though species-specific distribution models have been developed, they mainly focused on the ecological requirements related to climate (e.g., Guisan and Thuiller, 2005; Guisan et al., 2006, 2013; Zimmermann and Kienast, 1999).

However, the capability of vegetation as an ecological indicator of displacement depends on the type of process and on the depth of the displacement within the ground/soil and its interaction with the rooting zone. Our data confirm that the occurrence of single plant species (such as *Geum reptans*, *Cerastium uniflorum*, *Veronica alpina*) and/or the coverage of vegetation is a suitable indicator of displacement and of its intensity when the movement/displacement exceeds the rooting zone (up to 70 cm for *Geum reptans*, between 10 and 35 cm for the other two species) and involves coarse material, such as in the case of most the active rock glaciers, or at the foot of scree slopes (e.g., Burga et al., 2004; Cannone and Gerdol, 2003). For this specific condition, the species highlighted as indicators of surface displacement are reported in Fig. 4. Our data show that the mean surface displacement of the vegetation polygons (that are good representative of the vegetation relevés) is in a good relationship with the surface displacement modelled at the relevés locations for the 0–35 cm zone ($R^2 = 0.78$, $p < 0.001$).

In the areas with prevailing fine material and displacement depth exceeding the rooting zone depth, our data show that in this specific condition the occurrence of floating patches of continuous vegetation cover dominated by graminoids can be used as indicator of high deep displacements (such as for solifluction or creep processes). In this case, the patches/turves are mainly characterized by high total cover and by the dominance of graminoids (such as *Luzula alpino-pilosa, Poa alpina, Carex curvula, Anthoxanthum alpinum, Agrostis alpina),* creating a thick matrix of fasciculate roots, and/or by species able to perform clonal growth (Reisigl and Keller, 1990).

The wide range of geomorphological processes triggering the displacements addressed by this study (e.g., solifluction, frost creep, permafrost creep, slope wash, rockfalls, frost heave and so on) and their different depths allow to explain why the good ecological validation of our model is independent of the total vegetation coverage.

The total vegetation cover could be associated to the activity of specific landforms (Cannone and Gerdol, 2003), but, in case of broader areas, the interaction of many geomorphic processes and substrata produce a heterogeneous disturbance system even at similar coverages.

Nevertheless, it is important to remark that the displacement-tolerant species found in this study are not exclusive of unstable surfaces and thus they cannot be treated as the only ones to colonize displacing areas, rather they are able to grow also above disturbed surfaces.

6. Conclusions

A new simple topo-climatic model for predicting surficial dynamics in mountain regions was presented here showing that it is possible to develop and use linear models also for modeling the land evolution and degradation of alpine territories in the periglacial belt where permafrost is actually degrading.

Our findings suggest that slope and GHI are the best predictors of surficial displacement in the examined alpine area. In particular, the general regression model shows that steep zones with high GHI are more susceptible to undergo periglacial and paraglacial processes. As expected, slope is fundamental to trigger processes such as gravitation, nivation, solifluction and their interactions, but our model shows that GHI (that is the amount of energy transferred to the ground) is fundamental too. GHI highlights the role of climate in controlling the surface displacement, because in areas where GHI is higher, the ground can stay snow-free for a longer time and therefore, can be affected by liquid precipitation and, consequently more runoff or slopewash (Thorn and Hall, 2002). Moreover, in the same areas a more rapid snow melting can result in saturated deposits and therefore solifluction or mass movement processes may occur.

According to the available data for permafrost, we can confirm that in the periglacial belt the largest displacements were detected where permafrost degradation occurred since 1990 (and probably is still ongoing) and could remain one of the main triggering factors for future surface displacements.

An ecological implication of the model is possible for surface displacements >35 cm especially where coarse material occurs on the surface, such as on coarse active rock glaciers and screes. Such areas may act as physical barriers to the grassland species not adapted to the surface displacement, which are trying to shift towards higher altitude in response to climate warming. Therefore, an increase of surface displacement can contribute to the loss of grassland species threatened by shrub encroachment from lower elevation sand by the increase of the surficial displacement in their potential refugial areas located at higher elevations. When the surficial material is fine, displacements deeper than the rooting zone allow the development of discontinuous vegetation with high cover and dominated by graminoids forming patches floating above the displacement plane. When the displacement is surficial, vegetation creates small discontinuous turves of consolidator species (such as graminoids) able to survive being buried by fine material. Plant species apparently not indicators of movement (such as graminoids) in specific geomorphic conditions can develop also with large surface displacements and therefore the combination of surface displacement type (deep vs surficial), material texture (fine vs coarse) and vegetation cover (high vs low) and floristic composition can be used as a valuable ecological indicator of movement.

Our results suggest that both landscape degradation and vegetation displacement can be very fast especially where the air warming has been notable as in the selected study area. Therefore, in order to predict future surface displacements, we suggest adopt a monitoring of the ground surface temperature (2 cm of depth) especially in the areas close to the lower altitudinal boundaries of permafrost distribution. Such monitoring is quite easily undertaken through the *in situ* placement of low cost dataloggers or with remote sensing technique (thermal imaging) or alternatively with the application of the model presented here.

CRediT authorship contribution statement

Ponti Stefano: Formal analysis, Methodology, Investigation, Validation, Writing - original draft, Software, Data curation, Visualization. **Cannone Nicoletta:** Conceptualization, Supervision, Funding acquisition, Formal analysis, Methodology, Investigation, Validation, Writing - original draft, Writing - review & editing. **Guglielmin Mauro:** Conceptualization, Supervision, Funding acquisition, Methodology, Investigation, Validation, Writing - original draft, Writing - review & editing.

Declaration of Competing Interest

The authors declare that they have no known competing financial interests or personal relationships that could have appeared to influence the work reported in this paper.

Acknowledgments

We acknowledged the project that funded this research that is the Project PRIN “RESACC” and the id of the grant is 2015N8F555. The Funder is MIUR (Ministery of University and Research).

We thank the Stelvio National Park for logistical and financial support to our work. We want also to thank you the two anonymous reviewers that improved a lot the paper.

Appendix A. Supplementary data

Supplementary data to this article can be found online at https://doi.org/10.1016/j.ecolind.2020.106889.

References

Aalto, J., Luoto, M., 2014. Integrating climate and local factors for geomorphological distribution models. Earth Surf. Proc. Land. 39, 1729–1740. https://doi.org/10.1002/esp.3554.

Arenson, L.U., Kääb, A., O'Sullivan, A., 2016. Detection and analysis of ground deformation in permafrost environments. Permafrost Periglac. Process. 27, 339–351. https://doi.org/10.1002/ppp.1932.

Baas, A.C.W., 2013. Quantitative Modeling of Geomorphology, in: Shroder, J.F. (Ed.), Treatise on Geomorphology (Vol. 2). San Diego, pp. 1-5. https://doi.org/10.1016/b978-0-12-374739-6.00023-3.

Bai, S.B., Wang, J., Lü, G.N., Zhou, P.G., Hou, S.S., Xu, S.N., 2010. GIS-based logistic regression for landslide susceptibility mapping of the Zhongxian segment in the Three Gorges area China. Geomorphology 115, 23–31. https://doi.org/10.1016/j.geomorph.2009.09.025.

Ballantyne, C.K., 1985. Nivation landforms and snowpatch erosion on two massifs in the Northern Highlands of Scotland. Scott. Geogr. Mag. 101, 40–49. https://doi.org/10.1080/14702548508553814.

Ballantyne, C.K., 2013. A 35-Year Record of Solifluction in a Maritime Periglacial Environment. Permafrost Periglac. Process. 24, 56–66. https://doi.org/10.1002/ppp.1761.

Becker, A., Bugmann, H., 1997. Predicting global change impacts on mountain hydrology and ecology: integrated catchment hydrology/altitudinal gradient studies. Workshop Report: Documentation Resulting from an International Workshop: Kathmandu, Nepal, 30 March 1996. Global Change Report (Sweden).

Benedict, J.B., 1970. Downslope soil movement in a Colorado alpine region: rates, processes, and climatic significance. Arct. Alp. Res. 2, 165–226. https://doi.org/10.2307/1550306.

Boeckli, L., Brenning, A., Gruber, S., Noetzli, J., 2012a. Permafrost distribution in the European Alps: calculation and evaluation of an index map and summary statistics. The Cryosphere 6, 807. https://doi.org/10.5194/tcd-6-849-2012.

Boeckli, L., Brenning, A., Gruber, S., Noetzli, J., 2012b. A statistical approach to modelling permafrost distribution in the European Alps or similar mountain ranges. Cryosphere 6, 125–140. https://doi.org/10.5194/tc-6-125-2012.

Brenning, A., 2005. Spatial prediction models for landslide hazards: review, comparison and evaluation. Natural Hazards and Earth System Science. 5, 853–862. https://doi.org/10.5194/nhess-5-853-2005.

Burga, C.A., Frauenfelder, R., Ruffet, J., Hoelzle, M., KääB, A., 2004. Vegetation on Alpine rock glacier surfaces: A contribution to abundance and dynamics on extreme plant habitats. Flora-Morphol. Distrib. Funct. Ecol. Plants. 199, 505–515. https://doi.org/10.1078/0367-2530-00179.

Cai, Q.G., Zhu, Y.D., Wang, S.Y., 2004. Research on processes and factors of rill erosion. Adv. Water Sci. 15, 18–22.

Cannone, N., Gerdol, R., 2003. Vegetation as an ecological indicator of surface instability in rock glaciers. Arct. Antarct. Alp. Res. 35, 384–390. https://doi.org/10.1890/1540-9295(2007)5[360:UIOCCO]2.0.CO;2.

Cannone, N., Guglielmin, M., Hauck, C., Vonder Muhll, D. 2003. The impact of recent glacier fluctuation and human activities on the permafrost distribution: a case study from Stelvio Pass (Italian Central-Eastern Alps). In: Editors M. Phillips, S. M. Springman, L. U. Arenson. PERMAFROST - ICOP 2003 (International Conference On Permafrost 2003). Zurigo, 21 – 25 July 2003, vol. 1, p. 137-143, LISSE:Balkema, ISBN: 90-5809-582-7.

Cannone, N., Sgorbati, S., Guglielmin, M., 2007. Unexpected impacts of climate change on alpine vegetation. Front. Ecol. Environ. 5, 360–364. https://doi.org/10.1890/060141.

Cannone, N., Lewkowicz, A.G., Guglielmin, M., 2010. Vegetation colonization of permafrost-related landslides, Ellesmere Island, Canadian high arctic. J. Geophys. Res. Biogeosci. 115 (G4) https://doi.org/10.1029/2010JG001384.

Cannone, N., Guglielmin , M., Ponti, S. (in prep). Surface displacement lost its effect as physical barrier against climate driven upslope migration of low elevation species.

Carrara, A., Crosta, G., Frattini, P., 2008. Comparing models of debris-flow susceptibility in the alpine environment. Geomorphology 94, 353–378. https://doi.org/10.1016/j.geomorph.2006.10.033.

Carter, T.R., Porter, J.H., Parry, M.L., 1991. Climatic warming and crop potential in Europe: prospects and uncertainties. Global Environ. Change 1, 291–312. https://doi.org/10.1016/0959-3780(91)90056-y.

Ceriani, M., Carelli, M., 2000. Carta delle precipitazioni medie, massime e minime annue del territorio alpino della Regione Lombardia (registrate nel periodo 1891–1990). Servizio Geologico, Ufficio Rischi Geologici Regione Lombardia.

Chapin, F.S., Randerson, J.T., McGuire, A.D., Foley, J.A., Field, C.B., 2008. Changing feedbacks in the climate-biosphere system. Front. Ecol. Environ. 6, 313–320. https://doi.org/10.1890/080005.

Choudhary, K., Boori, M.S., Kupriyanov, A., 2017. Spatial modelling for natural and environmental vulnerability through remote sensing and GIS in Astrakhan, Russia. Egypt. J. Remote Sens. Space Sci. 21, 139–147. https://doi.org/10.1016/j.ejrs.2017.05.003.

Chung, C.J.F., Fabbri, A.G., 2003. Validation of spatial prediction models for landslide hazard mapping. Nat. Hazards 30, 451–472. https://doi.org/10.1023/b:nhaz.0000007172.62651.2b.

Coulthard, T.J., 2001. Landscape evolution models: A software review. Hydrol. Process. 15, 165–173. https://doi.org/10.1002/hyp.426.

Das, I., Sahoo, S., van Westen, C., Stein, A., Hack, R., 2010. Landslide susceptibility assessment using logistic regression and its comparison with a rock mass classification system, along a road section in the northern Himalayas (India). Geomorphology 114, 627–637. https://doi.org/10.1016/j.geomorph.2009.09.023.

Diolaiuti, G.A., Maragno, D., D'Agata, C., Smiraglia, C., Bocchiola, D., 2011. Glacier retreat and climate change: Documenting the last 50 years of Alpine glacier history from area and geometry changes of Dosde Piazzi glaciers (Lombardy Alps, Italy). Prog. Phys. Geogr. 35, 161–182. https://doi.org/10.1177/0309133311399494.

Draebing, D., Eichel, J., 2018. Divergence, convergence, and path dependency of paraglacial adjustment of alpine lateral moraine slopes. Land Degrad. Dev. 29 (6), 1979–1990. https://doi.org/10.1002/ldr.2983.

Dymond, J.R., Ausseil, A.G., Shepherd, J.D., Buettner, L., 2006. Validation of a region-wide model of landslide susceptibility in the Manawatu-Wanganui region of New Zealand. Geomorphology 74, 70–79. https://doi.org/10.1016/j.geomorph.2005.08.005.

Ellenberg, H.H., 1988. Vegetation ecology of central Europe. Cambridge University Press.

ESRI (Environmental Systems Research Institute), 2011. ArcGIS Desktop: Release 10. Environmental Systems Research Institute Inc., Redlands, CA.

Frattini, P., Crosta, G., Carrara, A., Agliardi, F., 2008. Assessment of rockfall susceptibility by integrating statistical and physically-based approaches. Geomorphology 94, 419–437. https://doi.org/10.1016/j.geomorph.2006.10.037.

French, H.M., 2007. The periglacial environment, third ed. Wiley and Sons, Chichester, UK. https://doi.org/10.1002/9781118684931.

Fronzek, S., Luoto, M., Carter, T.R., 2006. Potential effect of climate change on the distribution of palsa mires in subarctic Fennoscandia. Clim. Res. 32, 1–12. https://doi.org/10.3354/cr032001.

Giacomini, V., Pignatti, S., 1955. Flora e vegetazione dell'alta valle del Braulio con speciale riferimento ai pascoli di altitudine. Fondazione per i Problemi Montani dell'Arco Alpino.

Goodfellow, B.W., Boelhouwers, J., 2013. Hillslope processes in cold environments: an illustration of high-latitude mountain and hillslope processes and forms, in: Shroder, J.F. (Ed.), Treatise on Geomorphology (Vol. 2). San Diego, pp. 1-5. doi:10.1016/b978-0-12-374739-6.00181-0.

Gottfried, M., Pauli, H., Futschik, A., Akhalkatsi, M., Barancok, P., Alonso, J.L.B., Krajci, J., 2012. Continent-wide response of mountain vegetation to climate change. Nat. Clim. Change 2, 111. https://doi.org/10.1038/nclimate1329.

Govers, G., 1992. Relationship between discharge, velocity and flow area for rills eroding loose, non-layered materials. Earth Surf. Proc. Land. 17, 515–528. https://doi.org/10.1002/esp.3290170510.

Grab, S., 2001. Needle ice observations from the high Drakensberg Lesotho. Permafrost Periglacial Process. 12, 227–231. https://doi.org/10.1002/ppp.371.

Guglielmin, M., 2004. Observations on permafrost ground thermal regimes from Antarctica and the Italian Alps, and their relevance to global climate change. Global Planet. Change 40, 159–167. https://doi.org/10.1016/s0921-8181(03)00106-1.

Guglielmin, M., Tellini, C., 1992. Contributo alla conoscenza dei rock glaciers delle Alpi Italiane. I rock glaciers del Livignasco (Alta Valtellina, Sondrio). Rivista Geografica Italiana 99, 395–414.

Guglielmin, M., Siletto, G.B., 2000. Carta della criosfera. Regione Lombardia, Edilizia Residenziale, Firenze.

Guglielmin, M., Cannone, N., Dramis, F., 2001. Permafrost-glacial evolution during the Holocene in the Italian Central Alps. Permafrost Periglac. Process. 12, 111–124. https://doi.org/10.1002/ppp.379.

Guglielmin, M., Aldighieri, B., Testa, B., 2003. PERMACLIM: a model for the distribution of mountain permafrost, based on climatic observations. Geomorphology 51, 245–257. https://doi.org/10.1016/s0169-555x(02)00221-0.

Guglielmin, M., Donatelli, M., Semplice, M., Serra Capizzano, S., 2018. Ground surface temperature reconstruction for the last 500 years obtained from permafrost temperatures observed in the SHARE STELVIO Borehole, Italian Alps. Climate Past. 14, 709–724. https://doi.org/10.5194/cp-14-709-2018.

Guisan, A., Thuiller, W., 2005. Predicting species distribution: offering more than simple habitat models. Ecol. Lett. 8, 993–1009. https://doi.org/10.1111/j.1461-0248.2005.00792.x.

Guisan, A., Lehmann, A., Ferrier, S., Austin, M., Overton, J., Aspinall, R., Hastie, T., 2006. Making better biogeographical predictions of species' distributions. J. Appl. Ecol. 43, 386–392. https://doi.org/10.1111/j.1365-2664.2006.01164.x.

Guisan, A., Tingley, R., Baumgartner, J.B., Naujokaitis-Lewis, I., Sutcliffe, P.R., Tulloch, A.I., Martin, T.G., 2013. Predicting species distributions for conservation decisions. Ecol. Lett. 16, 1424–1435. https://doi.org/10.1111/ele.12189.

Haeberli, W., Hallet, B., Arenson, L., Elconin, R., Humlum, O., Kääb, A., Mühll, D.V., 2006. Permafrost creep and rock glacier dynamics. Permafrost Periglac. Process. 17, 189–214. https://doi.org/10.1002/ppp.561.

Harris, C., Rea, B., Davies, M., 2001. Scaled physical modelling of mass movement processes on thawing slopes. Permafrost Periglac. Process. 12, 125–135. https://doi.org/10.1002/ppp.373.

Harris, C., Smith, J.S., 2003. Modelling gelifluction processes: the significance of frost heave and slope gradient. In: Zurich. Swets and Zeitlinger, Lisse,, . (Ed.), Proceedings of the 8th International Conference on Permafrost, pp. 355–360.

Harris, S.A., Cheng, G., Zhao, X., Yongqin, D., 1998. Nature and dynamics of an active block stream, Kunlun Pass, Qinghai Province, People's Republic of China. Geografiska Annaler: Series A, Physical Geography. 80, 123–133. https://doi.org/10.1111/1468-0459.00031.

Hill, T., Lewicki, P., Lewicki, P., 2006. Statistics: methods and applications: a comprehensive reference for science, industry, and data mining. StatSoft Inc., 832 pp.

Hjort, J., 2014. Which environmental factors determine recent cryoturbation and solifluction activity in a subarctic landscape? A comparison between active and inactive features. Permafrost Periglac. Process. 25, 136–143. https://doi.org/10.1002/ppp.1808.

Hjort, J., Luoto, M., Seppälä, M., 2007. Landscape scale determinants of periglacial features in subarctic Finland: a grid-based modelling approach. Permafrost Periglac. Process. 18, 115–127. https://doi.org/10.1002/ppp.584.

IPCC, 2013. Climate Change 2013: the Physical Science Basis: Working Group I Contribution to the Fifth Assessment Report of the Intergovernmental Panel on Climate Change. Cambridge University Press, United Kingdom and New York, USA. Available at: http://www.ipcc.ch/report/ar5/wg1/.

Kääb, A., Haeberli, W., Gudmundsson, G.H., 1997. Analysing the creep of mountain permafrost using high precision aerial photogrammetry: 25 years of monitoring Gruben rock glacier. Swiss Alps. Permafrost Periglacial Process. 8, 409–426. https://doi.org/10.1002/(sici)1099-1530(199710/12)8:4%3C409::aid-ppp267%3E3.0.co;2-c.

Kääb, A., Kaufmann, V., Ladstädter, R., Eiken, T., 2003. Rock glacier dynamics: Implications from high-resolution measurements of surface velocity fields. Eighth Int. Conf. Permafrost 1, 501–506.

Kääb, A., Girod, L.M.R., Berthling, I.T., 2014. Surface kinematics of periglacial sorted circles using structure-from-motion technology. Cryosphere 8, 1041–1056. https://doi.org/10.5194/tc-8-1041-2014.

Keller, F., Kienast, F., Beniston, M., 2000. Evidence of response of vegetation to environmental change on high-elevation sites in the Swiss Alps. Reg. Environ. Change 1, 70–77. https://doi.org/10.1007/pl00011535.

Keller, F., Goyette, S., Beniston, M., 2005. Sensitivity analysis of snow cover to climate change scenarios and their impact on plant habitats in alpine terrain. Clim. Change 72, 299–319. https://doi.org/10.1007/s10584-005-5360-2.

Komac, M., 2006. A landslide susceptibility model using the analytical hierarchy process method and multivariate statistics in perialpine Slovenia. Geomorphology 74, 17–28. https://doi.org/10.1016/j.geomorph.2005.07.005.

Lee, S., 2005. Application of logistic regression model and its validation for landslide susceptibility mapping using GIS and remote sensing data. Int. J. Remote Sens. 26, 1477–1491. https://doi.org/10.1080/01431160412331331012.

Luckman, B.H., 1976. Rockfalls and rockfall inventory data: some observations from Surprise Valley, Jasper National Park Canada. Earth Surf. Process. Landforms 1, 287–298. https://doi.org/10.1002/esp.3290010309.

Luoto, M., Hjort, J., 2004. Generalized linear modelling in periglacial studies: Terrain parameters and patterned ground. Permafrost Periglac. Process. 15, 327–338. https://doi.org/10.1002/ppp.482.

Luoto, M., Hjort, J., 2005. Evaluation of current statistical approaches for predictive geomorphological mapping. Geomorphology 67 (3–4), 299–315. https://doi.org/10.1016/j.geomorph.2004.10.006.

Malfasi, F., Cannone, N., 2020. Climate warming persistence triggered tree ingression after shrub encroachment in a high alpine tundra. Ecosystems. https://doi.org/10.1007/s10021-020-00495-7.

Marmion, M., Hjort, J., Thuiller, W., Luoto, M., 2008. A comparison of predictive methods in modelling the distribution of periglacial landforms in Finnish Lapland. Earth Surf. Proc. Land. 33, 2241–2254. https://doi.org/10.1002/esp.1695.

Matsuoka, N., 1998. Modelling frost creep rates in an alpine environment. Permafrost Periglac. Process. 9, 397–409. https://doi.org/10.1002/(sici)1099-1530(199810/12)9:4%3C397::aid-ppp302%3E3.0.co;2-q.

Matsuoka, N., 2001a. Solifluction rates, processes and landforms: A global review. Earth Sci. Rev. 55, 107–134. https://doi.org/10.1016/s0012-8252(01)00057-5.

Matsuoka, N., 2001b. Direct observation of frost wedging in alpine bedrock. Earth Surf. Proc. Land. 26, 601–614. https://doi.org/10.1002/esp.208.

Matsuoka, N., 2006. Monitoring periglacial processes: Towards construction of a global network. Geomorphology 80, 20–31. https://doi.org/10.1016/j.geomorph.2005.09.005.

Messenzehl, K., Meyer, H., Otto, J.C., Hoffmann, T., Dikau, R., 2017. Regional-scale controls on the spatial activity of rockfalls (Turtmann valley, Swiss Alps) – A multivariate modeling approach. Geomorphology 287, 29–45. https://doi.org/10.1016/j.geomorph.2016.01.008.

Miao, C.Y., Yang, L., Chen, X.H., Gao, Y., 2012. The vegetation cover dynamics (1982–2006) in different erosion regions of the Yellow River basin China. Land Degradation Develop. 23, 62–71. https://doi.org/10.1002/ldr.1050.

Micheletti, N., Lambiel, C., Lane, S.N., 2015. Investigating decadal-scale geomorphic dynamics in an alpine mountain setting. J. Geophys. Res. Earth Surf. 120, 2155–2175. https://doi.org/10.1002/2015jf003656.

Miller, A.J., 2013. Assessing landslide susceptibility by incorporating the surface cover index as a measurement of vegetative cover. Land Degrad. Dev. 24, 205–227. https://doi.org/10.1002/ldr.1115.

Mod, H.K., Scherrer, D., Luoto, M., Guisan, A., 2016. What we use is not what we know: Environmental predictors in plant distribution models. J. Veg. Sci. 27, 1308–1322. https://doi.org/10.1111/jvs.12444.

Montrasio, A., Berra, F., Sciesa, E., Mazzoccola, D., Mair, V., Longhin, M., Arzuffi, L., 2012. Foglio 024 Bormio. Carta Geologica d'Italia alla scala 1 (50), 000.

Necsoiu, M., Onaca, A., Wigginton, S., Urdea, P., 2016. Rock glacier dynamics in Southern Carpathian Mountains from high-resolution optical and multi-temporal SAR satellite imagery. Remote Sens. Environ. 177, 21–36. https://doi.org/10.1016/j.rse.2016.02.025.

Nel, W., Boelhouwers, J., 2014. First observations on needle ice formation in the sub-Antarctic. Antarct. Sci. 26, 327. https://doi.org/10.1017/s0954102013000722.

Notarnicola, C., Duguay, M., Moelg, N., Schellenberger, T., Tetzlaff, A., Monsorno, R., Zebisch, M., 2013a. Snow cover maps from MODIS images at 250 m resolution, Part 1: Algorithm description. Remote Sens. 5, 110–126. https://doi.org/10.3390/rs5010110.

Notarnicola, C., Duguay, M., Moelg, N., Schellenberger, T., Tetzlaff, A., Monsorno, R., Zebisch, M., 2013b. Snow cover maps from MODIS images at 250 m resolution, part 2: Validation. Remote Sensing. 5, 1568–1587. https://doi.org/10.3390/rs5041568.

Oerlemans, J., 2005. Extracting a climate signal from 169 glacier records. Science 308, 675–677. https://doi.org/10.1126/science.1107046.

Paul, F., Kääb, A., Haeberli, W., 2007. Recent glacier changes in the Alps observed by satellite: Consequences for future monitoring strategies. Global Planet. Change 56, 111–122. https://doi.org/10.1016/j.gloplacha.2006.07.007.

Pelfini, M., 1992. Le fluttuazioni glaciali oloceniche nel Gruppo Ortles-Cevedale (settore lombardo). Università degli Studi di Milano. Dipartimento di Scienze della Terra (Doctoral dissertation, Tesi di Dottorato IV ciclo).

Pelletier, J.D., 2008. Quantitative modeling of earth surface processes. Cambridge. https://doi.org/10.1017/cbo9780511813849.009.

Pérez, F.L., 1993. Talus movement in the high equatorial Andes: A synthesis of ten years of data. Permafrost Periglac. Process. 4, 199–215. https://doi.org/10.1002/ppp.3430040303.

Pfeffer, K., Pebesma, E.J., Burrough, P.A., 2003. Mapping alpine vegetation using vegetation observations and topographic attributes. Landscape Ecol. 18, 759–776. https://doi.org/10.1023/b:land.0000014471.78787.d0.

Ponti, S., Cannone, N., Guglielmin, M., 2018. Needle ice formation, induced frost heave, and frost creep: A case study through photogrammetry at Stelvio Pass (Italian Central Alps). Catena. 164, 62–70. https://doi.org/10.1016/j.catena.2018.01.009.

Pradhan, B., 2010. Remote sensing and GIS-based landslide hazard analysis and cross-validation using multivariate logistic regression model on three test areas in Malaysia. Adv. Space Res. 45, 1244–1256. https://doi.org/10.1016/j.asr.2010.01.006.

Randin, C.F., Vuissoz, G., Liston, G.E., Vittoz, P., Guisan, A., 2009. Introduction of snow and geomorphic disturbance variables into predictive models of alpine plant distribution in the Western Swiss Alps. Arct. Antarct. Alp. Res. 41, 347–361. https://doi.org/10.1657/1938-4246-41.3.347.

Räsänen, A., Kuitunen, M., Hjort, J., Vaso, A., Kuitunen, T., Lensu, A., 2016. The role of landscape, topography, and geodiversity in explaining vascular plant species richness in a fragmented landscape. Boreal Environ. Res. 21, 53–70.

Reisigl, H., Keller, R., 1990. Fiori e ambienti delle Alpi. Editrice Saturnia, Trento, p. 148.

Rixhon, G., Demoulin, A., 2013. Evolution of slopes in a cold climate. Glacial and Periglacial Geomorphology, San Diego.

Saito, H., Nakayama, D., Matsuyama, H., 2009. Comparison of landslide susceptibility based on a decision-tree model and actual landslide occurrence: The Akaishi Mountains Japan. Geomorphology 109, 108–121. https://doi.org/10.1016/j.geomorph.2009.02.026.

Stanchi, S., Freppaz, M., Godone, D., Zanini, E., 2013. Assessing the susceptibility of alpine soils to erosion using soil physical and site indicators. Soil Use Manag. 29, 586–596. https://doi.org/10.1111/sum.12063.

Statham, I., 1976. A scree slope rockfall model. Earth Surf. Proc. Land. 1, 43–62. https://doi.org/10.1002/esp.3290010106.

Tharp, T.M., 1987. Conditions for crack propagation by frost wedging. Geol. Soc. Am. Bull. 99, 94–102. https://doi.org/10.1130/0016-7606(1987)99<94:cfcpbf>2.0.co;2.

Theurillat, J.P., Guisan, A., 2001. Potential impact of climate change on vegetation in the European Alps: A review. Clim. Change 50, 77–109. https://doi.org/10.1023/a:1010632015572.

Thorn, C.E., Hall, K., 2002. Nivation and cryoplanation: The case for scrutiny and integration. Prog. Phys. Geogr. 26, 533–550. https://doi.org/10.1191/0309133302pp351ra.

Tucker, G.E., Hancock, G.R., 2010. Modelling landscape evolution. Earth Surf. Proc. Land. 35, 28–50. https://doi.org/10.1002/esp.1952.

van den Bergh, T., Inauen, N., Hiltbrunner, E., Körner, C., 2013. Climate and plant cover co-determine the elevational reduction in evapotranspiration in the Swiss Alps. J. Hydrol. 500, 75–83. https://doi.org/10.1016/j.jhydrol.2013.07.013.

van Steijn, H., Boelhouwers, J., Harris, S., Hétu, B., 2002. Recent research on the nature, origin and climatic relations of blocky and stratified slope deposits. Prog. Phys. Geogr. 26, 551–575. https://doi.org/10.1191/0309133302 pp352ra.

Virtanen, R., Luoto, M., Rämä, T., Mikkola, K., Hjort, J., Grytnes, J.A., Birks, H.J.B., 2010. Recent vegetation changes at the high-latitude tree line ecotone are controlled by geomorphological disturbance, productivity and diversity. Glob. Ecol. Biogeogr. 19, 810–821. https://doi.org/10.1111/j.1466-8238.2010.00570.x.

Walther, G.R., Beißner, S., Burga, C.A., 2005. Trends in the upward shift of alpine plants. J. Veg. Sci. 16, 541–548. https://doi.org/10.1111/j.1654-1103.2005.tb02394.x.

Westermann, S., Duguay, C.R., Grosse, G., Kääb, A., 2015. Remote sensing of permafrost and frozen ground. Remote Sens. Cryosphere 1, 307–344. https://doi.org/10.1002/9781118368909.ch13.

Wieser, G., Hammerle, A., Wohlfahrt, G., 2008. The water balance of grassland ecosystems in the Austrian Alps. Arct. Antarct. Alp. Res. 40, 439–445. https://doi.org/10.1657/1523-0430(07-039)[wieser]2.0.co;2.

Willmott, C.J., 1981. On the validation of models. Phys. Geogr. 2 (2), 184–194. https://doi.org/10.1080/02723646.1981.10642213.

Zemp, M., Paul, F., Hoelze, M., Haeberli, W., 2008. Glacier fluctuations in the European Alps, 1850–2000. Darkening Peaks Glacier Retreat Sci, Soc.

Zimmermann, N.E., Kienast, F., 1999. Predictive mapping of alpine grasslands in Switzerland: species versus community approach. J. Veg. Sci. 10, 469–482. https://doi.org/10.2307/3237182.

Zinko, U., Seibert, J., Dynesius, M., Nilsson, C., 2005. Plant species numbers predicted by a topography-based groundwater flow index. Ecosystems 8, 430–441. https://doi.org/10.1007/pl00021513.